Available online at www.sciencedirect.com

ScienceDirect

Journal of Solid State Chemistry 180 (2007) 589–595

JOURNAL OF SOLID STATE CHEMISTRY

www.elsevier.com/locate/jssc

The relationship between the thermal expansions and structures of ABO_4 oxides

Huiling Li[a,b], Shihong Zhou[a], Siyuan Zhang[a,*]

[a]*Key Laboratory of Rare Earth Chemistry and Physics, Changchun Institute of Applied Chemistry, Chinese Academy of Sciences, Changchun 130022, PR China*

[b]*Graduate School of the Chinese Academy of Sciences, Beijing100049, China*

Received 10 August 2006; received in revised form 16 November 2006; accepted 16 November 2006
Available online 21 November 2006

Abstract

The linear thermal expansion coefficients of ABO_4 compounds are determined and the expansion tendency is analyzed from the chemical bond viewpoint. All chemical bonds contributions are involved. The contributions from different chemical bonds are compared with each other and the origin of the expansion behavior of ABO_4 oxides is revealed that the A–O bonds expansions dominate the compound expansion. The calculated expansion coefficients agree satisfactorily with the experimental data. By analyzing the expansion regularity the range of the expansion coefficients can be qualified. The thermal expansion coefficients of some ABO_4 compounds having not been measured are predicted and discussed.

Keywords: Thermal expansion; Crystal structure; Oxides

---

1. Introduction

Binary oxides with the general formula ABO_4, in which A and B cations can be multivalent and compositely substituted, have several common structure types. Many ABO_4 oxides, for example, silicates, phosphates, arsenates, vanadates and chromates are isostructural with zircon ($I4_1/amd$, No.141); several phosphates, arsendates occur as polymorphs of quartz; a few ABO_4 oxides, e.g., germinates, molybdates, tungstates and periodates crystallize in the scheelite structure ($I4_1/a$, No.88); a large number of molybdates, tungstates and tantalates crystallize with the wolframite structure ($P2/c$, No.13); relatively few ABO_4 oxides exist as M'-fergusonite structures ($P2_1/c$, No.14) or M'-fergusonite under normal conditions, but lots of ABO_4 oxides transform from zircon or scheelite structures to M'-fergusonite and M'-fergusonite under pressure; the fergusonite structure can be viewed as a distorted scheelite structure. A few ABO_4 oxides with A and B statistically distributed among the *2a* position such as in cassiterite (SnO_2) or *4c* position e.g., in α-PbO2, have tetragonal ($P4_2/mnm$, No.136) or orthorhombic (*Pbcn*, No.60) symmetry. The *Pnma* (No.62) phase is also a typical structure for ABO_4 oxides. Depero et al. provided more detailed information about the statistical distribution of the ABO_4 oxides structure types [1].

The A-, B-, and the O-ions in the zircon and scheelite structures show identical coordination environment, respectively. In these two structures, the A cations are surrounded by eight oxygen atoms with two different distances, the B cations coordinate with four oxygen atoms, and the oxygen anions are connected with two A-ion and one B-ion. However the BO_4 tetrahedra in zircon structure are less distorted than those in scheelite structure, moreover, the latter structure is more densely packed than the former. Compared with zircon structure, the scheelite structure is characterized by the layered stacked cell and so it can be readily distinguished from the other structures exhibited by ABO_4 oxides, the representative illustrations characterized the structures of ABO_4 oxides displayed in Figs. 1–3. The layered stacked cell of scheelite-type ABO_4 oxides is reflected in general larger c-axis parameter relative to other non-layered

---

*Corresponding author. Fax: +86 431 5698041.
E-mail address: syzhang@ciac.jl.cn (S. Zhang).

0022-4596/$ - see front matter © 2006 Elsevier Inc. All rights reserved.
doi:10.1016/j.jssc.2006.11.023

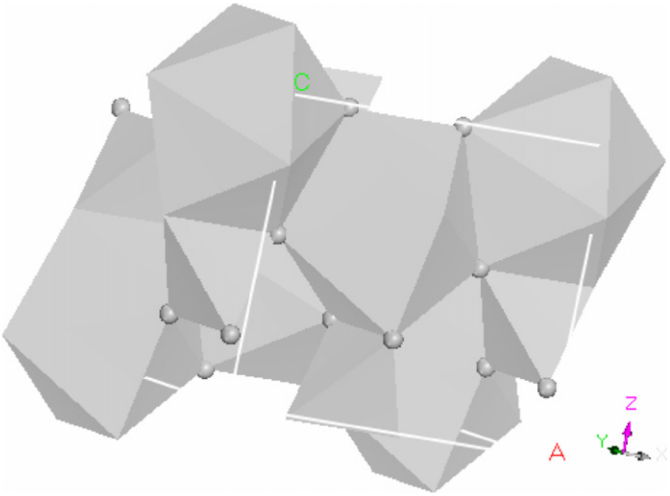

Fig. 1. Crystal of $CaCrO_4$ (zircon-type).

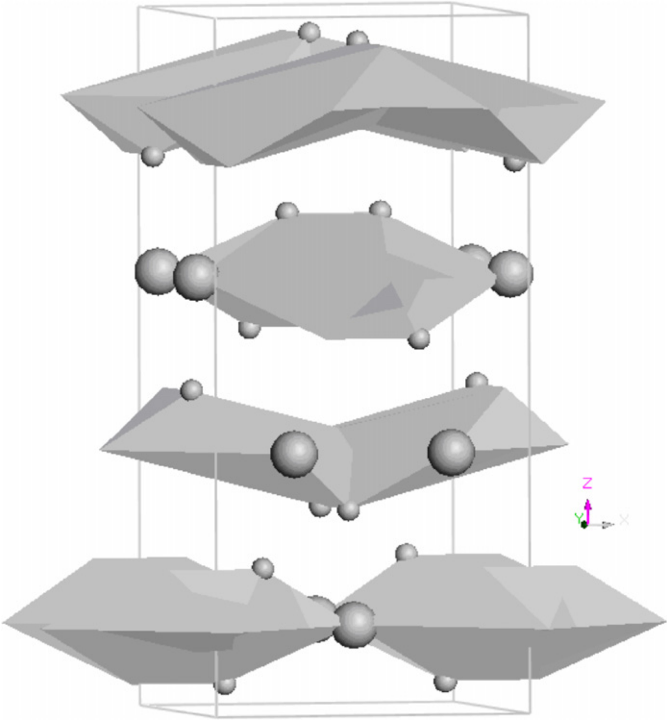

Fig. 2. Crystal structure of $CaWO_4$ (scheelite-type).

structures. The *A*- and *B*-cation of *AB*O_4 oxides belonged to space group No.12, No.13, and No.60 as well as No.136 structures are all sixfold coordinated with the oxygen atoms; the *B* cation in No.62 space group structure likewise is surrounded by six oxygen atoms, but the coordination anions around *A* cation in No.62 space group structure can fluctuate between eight and twelve. The largest cation coordination is in the $LaTaO_4$-type structure, the nearest-neighbor oxygen atoms of the *A*- and *B*-cation are eight and six, respectively. The *A* cation polyhedra in fergusonite-type structure (No.15) are alike to the $LaTaO_4$-type structure.

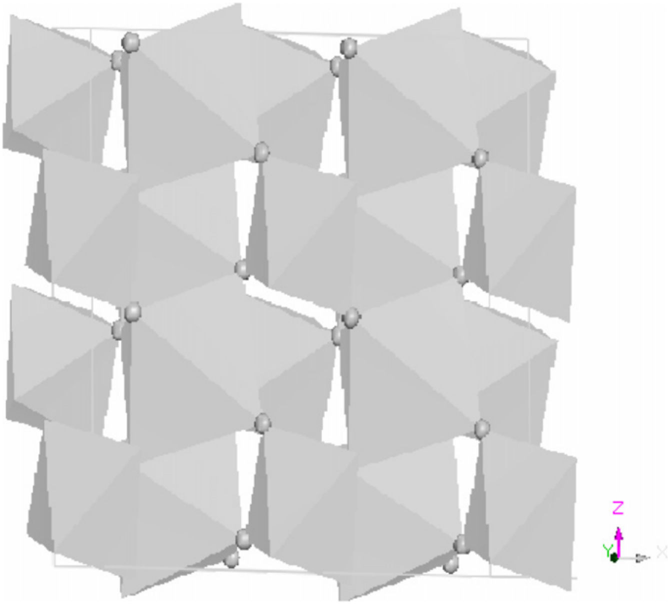

Fig. 3. Crystal structure of $CdWO_4$ (wolframite-type).

In view of the structure diversity and the *A*- and *B*-ions variety and the various properties and applications, *AB*O_4 oxides are important materials from both theoretical and technological standpoints. As a basic thermophysical property the thermal expansion behaviors of *AB*O_4 compounds are widely needed, whereas much investigation focused on compounds within limited structure types and until recently there is first principle simulation on the thermal expansion behavior of $CaWO_4$ [2].

At present, there are only a few methods available for the prediction of coefficients of thermal expansion (CTEs) of materials, especially for complex compounds. In view of quantum picture of solids, the thermal expansion depends on lattice-dynamical behaviors of solids. The basic theory of lattice vibrations dates back to the treatise of Born and Huang [3]. As a matter of fact, the understanding of thermal expansion in terms of phonon is the most convincing. The early Einstein model and Debye model can be used to attain the phonon dispersions. *Ab initio* calculation can be used to obtain accurate phonon dispersions on a fine grid of wave vectors covering the entire Brillouin zone, from which the thermal expansion coefficients can be calculated [4–6]. Whereas knowledge of phonon frequencies alone is not sufficient to determine the force constants completely, in addition, the method requires large computational cost in determining the complete phonon spectrum for complex compounds and it is static, zero-temperature. *Ab initio* molecular-dynamics, the combination of molecular dynamics and density-functional theory [7] also contain information on the dynamics of the system, i.e., on phonon modes and can accounts for all the anharmonic effects in the system at high temperatures, and therefore it is used to determine

CTE [8,9]. However, the straightforward estimation of phonon frequencies from molecular-dynamics simulations suffers from a few problems. First, at low temperature all the systems are strongly harmonic and, hence, poorly ergodic. The time necessary to reach equilibrium may thus be impractically long. The second problem is that the results may depend on the size of the simulation (super)cell when molecular-dynamics simulations are used to predict the temperature dependence of vibrational modes and the thermal behavior of properties. As the computer workload of standard DFT calculations scales as the cube of the number of the atoms in the unit cell, the calculation is limited to semiconductors, simple metals, and simple oxides including some simple superconductors, as well as the special modes interested in superconductors. Except for empirical methods [10–15] the equation of state [16–20] can be applied to calculate CTE. But the fitting parameters are not usually transferable. There are still lack of systematic and completed research and analyses.

This paper presents a qualitative investigation of the thermal expansions of some ABO_4 oxides by means of chemical bond theory based on dielectric description. The coefficients of thermal expansion are determined from the contributions of all constituent chemical bonds in compounds, and the relationships between the thermal expansion properties and the structures will be analyzed and discussed.

2. Theoretical method

It is well known that the normal thermal expansions of crystals originate from the anharmonic behaviors in crystals. The volumes of the unit cells change as thermal expanding, and so the equilibrium distances between the atoms. In the expansion process, the binding interaction between ions must be conquered. Therefore, the larger the binding interaction, i.e. the stronger the bond, the smaller the expansion would be. Lattice energy is one of the major signals of the interaction strength between ions in crystals. So crystal with larger thermal expansion coefficient would have less lattice energy, i.e. the expansion coefficient should be inversely proportional to lattice energy. The method of calculating lattice energy was well established [21]. This makes it convenient for studying the relationship between the expansion coefficient and lattice energy.

According to the theory [21], the lattice energy of μ type of chemical bond $\left(A^i_{mi}B^j_{nj}\right)$ can be divided into the ionic (U^μ_{i}) and covalent (U^μ_{c}) component:

$$U^\mu = U^\mu_{\mathrm{i}} + U^\mu_{\mathrm{c}}. \tag{1}$$

The ionic part is given by

$$U^\mu_{\mathrm{i}} = \frac{1270 \times (mi+nj) \times Z^\mu_A \times Z^\mu_B}{d^\mu}\left(1-\frac{0.4}{d^\mu}\right) f^\mu_{\mathrm{i}} \quad (\mathrm{kJ\,mol^{-1}}), \tag{2}$$

where d^μ is the bond length of μ type of chemical bond, Z^μ_A is the valence of the A cation, f^μ_{i} is fractional ionicity of μ type of chemical bond.

The covalent part

$$U^\mu_{\mathrm{c}} = 2100mi\frac{(Z^\mu_{\mathrm{A}})^{1.64}}{(d^\mu)^{0.75}} f^\mu_{\mathrm{c}} \quad (\mathrm{kJ\,mol^{-1}}), \tag{3}$$

where f^μ_{c} is fractional covalency of μ type of bond.

Thus the thermal expansion coefficient can be evaluated from the following equations [22,23]:

$$\gamma^\mu = \frac{kN_A Z^\mu_A N^\mu_{CA}}{U^\mu \Delta^\mu}\beta^\mu \quad (10^{-6}\,\mathrm{K^{-1}}), \tag{4}$$

$$\beta^\mu = \frac{mi(mi+nj)}{2nj},$$

$$\alpha^\mu = -3.1685 \times 10^{-6} + 0.8376\gamma^\mu \quad (10^{-6}\,\mathrm{K^{-1}}), \tag{5}$$

$$\alpha = \sum_\mu F^\mu \alpha^\mu \quad (10^{-6}\,\mathrm{K^{-1}}), \tag{6}$$

where k is the Boltzmann constant, N_A is the Avogadro constant and Δ^μ_A is a correct factor related to the row of cation in the periodic table, F^μ_{mn} is the algebraic fraction of μ type of bond in the complex crystal. The thermal expansion magnitude determined by the strength of the interaction between atoms is expressed in Eq. (5). From the reciprocal relationship between γ^μ and U^μ, it confirms the expansion coefficient is inversely proportional to the lattice energy of the bond. The parameters (−3.1685 and 0.1876) in Eq. (5) are derived from fitting the experimental expansion coefficients with calculated γ values for I–VII,II–VI and III–V simple solids. In order to make the expression to be simple, the correlation is expressed separately in Eq. (4). While the expansion coefficients of chemical bonds are calculated, the average crystal expansion coefficient can be obtained regarding the statistical contribution of all the chemical bonds through Eq. (6).

3. Results and discussions

According to the dielectric chemical bond theory [21,24,25] and the crystallography data [26,27], the ABO_4 oxides in zircon and scheelite structures can be decomposed into the subformulas equation as

$$ABO_4 = A_{1/2}O_{4/3} + A_{1/2}O'_{4/3} + BO_{4/3}.$$

The decomposing equation ABO_4 oxides in wolframite structure can be written as [28]

$$\begin{aligned} ABO_4 &= ABO_2(1)O_2(2) \\ &= A_{2/3}O_{2/3}(1) + A_{2/3}O_{2/3}(1)' + A_{2/3}O_{2/3}(2) \\ &\quad + B_{1/3}O_{2/3}(1) + B_{2/3}O_{2/3}(2) + B_{2/3}O_{2/3}(2)'. \end{aligned}$$

The results of the calculated gamma values and the linear thermal expansion coefficients are summarized in Tables 1 and 2 and the developments against bond lengths are

Table 1
Chemical bonds properties of ABO_4 oxides, α_{cal} and α_{exp} denote calculated and experimental thermal expansion coefficients

Crystals	Chemical bonds	f_c^μ	U^μ(KJ/mol)	$\gamma^\mu(10^{-6}K^{-1})$	$\alpha^\mu(10^{-6}K^{-1})$	$\alpha_{cal}(10^{-6}K^{-1})$	$\alpha_{exp}(10^{-6}K^{-1})$	Error %	Refs.
$ZrSiO_4$(Z)	SiO	0.4209	15537	6.1	1.9	4.8	3.9	0.23	[39]
	ZrO	0.1169	5126	11.4	6.4				
	ZrO′	0.1203	5381	10.9	6.0				
$HfSiO_4$(Z)	SiO	0.4211	15550	6.1	1.9	4.1	3.6	0.14	[40]
	HfO	0.1171	5140	10.2	5.4				
	HfO′	0.1207	5412	9.7	5.0				
YPO_4(Z)	PO	0.3718	24647	4.8	0.9	6.7	5.9	0.14	[39]
	YO	0.1586	2845	15.5	9.8				
	YO′	0.1608	2917	15.1	9.5				
YVO_4(Z)	VO	0.3526	22978	4.4	0.5	6.7	6.7	0.0	[41]
	YO	0.1529	2786	15.8	10.0				
	YO′	0.1572	2924	15	9.4				
$YAsO_4$(Z)	AsO	0.3569	23315	4.3	0.4	6.6	6.6	0.0	[42]
	YO	0.1546	2806	15.7	10.0				
	YO′	0.1580	2915	15.1	9.5				
$ScPO_4$(Z)	PO	0.3689	24765	4.8	0.8	6.9	5.5	0.25	[42]
	ScO	0.1600	2957	16	10.2				
	ScO′	0.1640	3071	15.4	9.7				
$ScVO_4$(Z)	VO	0.3501	22776	4.4	0.5	6.9	7.4	−0.07	[41]
	ScO	0.1538	2835	16.7	10.8				
	ScO′	0.1653	3166	14.9	9.3				
$ScAsO_4$(Z)	AsO	0.3528	23337	4.3	0.4	6.9	5.8	0.21	[42]
	ScO	0.1554	2902	16.3	10.5				
	ScO′	0.1617	3085	15.3	9.7				
$CaCrO_4$(Z)	CrO	0.3165	33776	3.7	~0	11.3	11.7	−0.03	[40]
	CaO	0.2293	1280	24.6	17.5				
	CaO′	0.2353	1337	23.6	16.6				
$CaWO_4$(S)	WO	0.3304	31833	3.2	~0	11.2	12.6	−0.11	[32]
	CaO	0.2446	1297	24.3	17.2				
	CaO′	0.2464	1315	24	16.9				
$CaMoO_4$(S)	MoO	0.3304	31950	3.5	~0	11.3	13.1	−0.14	[32]
	CaO	0.2451	1304	24.1	17.1				
	CaO′	0.2458	1310	24	17.0				
$SrWO_4$(S)	WO	0.3347	31807	3.2	~0	10.8	8.3	0.30	[39]
	SrO	0.2425	1245	23.6	16.6				
	SrO′	0.2437	1257	23.3	16.4				
$BaWO_4$(S)	WO	0.3399	31734	3.2	~0	10.0	9.1	0.10	[43]
	BaO	0.2411	1184	22.2	15.4				
	BaO′	0.2423	1198	21.9	15.2				
$CdMoO_4$(S)	MoO	0.3314	32215	3.5	~0	10.2	12.0	−0.15	[39]
	CdO	0.2464	1315	22.3	15.5				
	CdO′	0.2483	1330	22	15.3				

illustrated in Figs. 4 and 5. The calculated lattice energies vs. *A*–O bond distances are displayed in Fig. 6 and compared with those estimated from the method of Glasser [29] in Table 3. From Table 1 and Figs. 5–7, it is obvious that in the same structure family, as the *A* cation valence increases, the *A*–O bond covalency decreases, the *A*–O bond lattice energy increases, the binding interaction becomes stronger, this means that the *A*–O bond strengthens, the average *A*–O bond expansion against the binding interaction decreases reasonably. The *B*–O bond parameters alter oppositely. For instance, while the *A* cation changes from Ca to Zr (Hf) and the *B* cation from Cr to Si, the *A*–O bond covalency drops from more than 20% down to about 10% and the *B*–O bond covalency rises from nearly 30% to 40%. The low covalencies of *A*–O and *B*–O bonds indicate that most of the bonds in ABO_4 principally ionic bonds in nature, which consists with the temperature and pressure dependence of Raman spectra of $CaMoO_4$ [30]. The covalency of Si–O bond in $ZrSiO_4$ is 0.4209. The calculated charge of Si in $ZrSiO_4$ by Guittet [31] is +1.93, compared with the formal charge of Si to be +4 while the ionicity of Si–O bond being 1.0, this suggested 48% ionic character of Si–O bond in $ZrSiO_4$. In view of the method of Guittet [31], the calculated charge of atoms is affected by the wave basis, the cutting-off energy and other parameters in the procedure. Therefore, the ionicity deduced from Guittet is consistent with the ionicity (0.5791) calculated by the present method. The average ionicity of Zr–O estimated by the present method to be 0.8814 is also close to the 0.7125 deduced from Ref. [31]. Therefore we can

Table 2
Predicted thermal expansion coefficients for ABO_4 oxides

Crystals	$\alpha_{cal}(10^{-6}\,K^{-1})$
$USiO_4$(Z)	4.5
$LuAsO_4$(Z)	5.6
$LuPO_4$(Z)	5.7
$TbCrO_4$(Z)	5.8
$SrMoO_4$(S)	10.9
$NiWO_4$(W)	5.4
$MgWO_4$(W)	6.7
$CoWO_4$(W)	5.5
$ZnWO_4$(W)	5.5
$FeWO_4$(W)	5.6
$MnWO_4$(W)	5.7
$CdWO_4$(W)	5.5
$KMnO_4$(*Pnma*)	27.8
$GaTaO_4$(*Pbcn*)	3.8
$CrVO_4$(*Cmcm*)	3.9
$AlTaO_4$(*C2/m*)	4.5
$HgMoO_4$(*C2/c*)	9.1

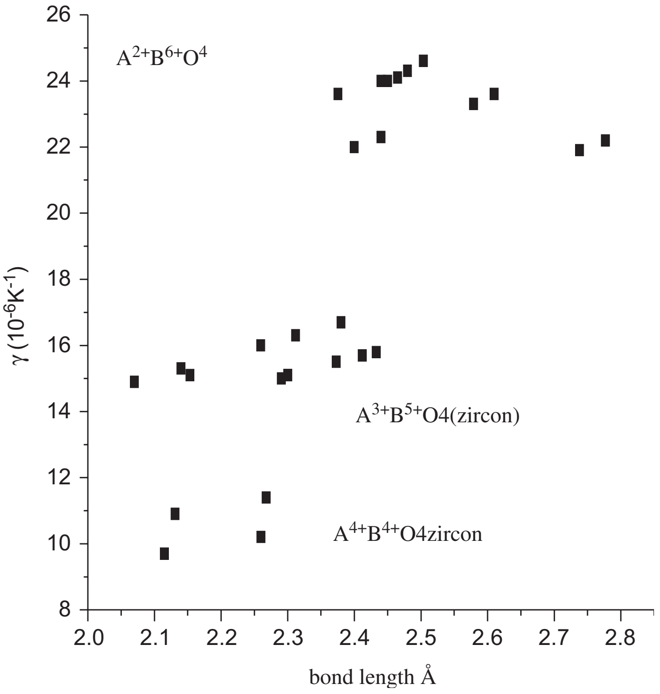

Fig. 4. The calculated gamma values of *A*–O bonds versus *A*–O bond lengths.

believe the validity of the covalencies given by the present paper. The ionic radius of Hf^{4+} (0.71 nm) is slightly smaller than the radius of Zr^{4+} (0.72). This will lead the bond covalency of Hf–O bond to be larger than Zr–O bond, and then the expansion coefficient of $HfSiO_4$ is somewhat smaller than that of $ZrSiO_4$. The calculation results agree with the general considerations. The *A*–O bond expansion decreases from 17 ($10^{-6}\,K^{-1}$) to 5.2 ($10^{-6}\,K^{-1}$) as the *A* cation changes from Ca to Zr (Hf) and the B cation from Cr to Si. The corresponding compounds thermal expansion

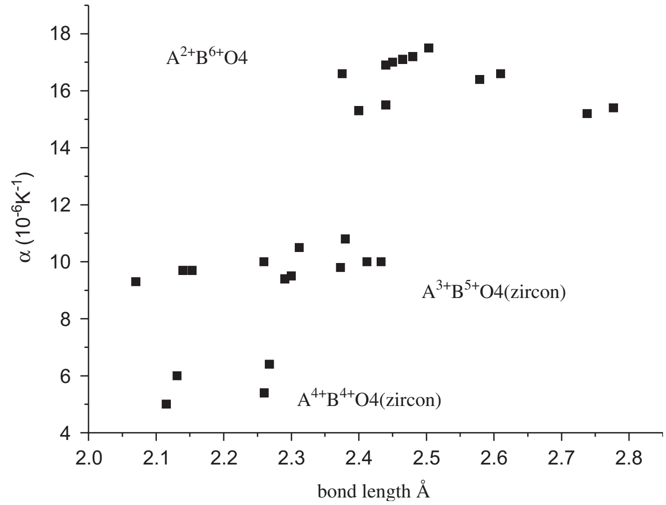

Fig. 5. The evaluated CTEs of *A*–O bonds change against *A*–O bond distances.

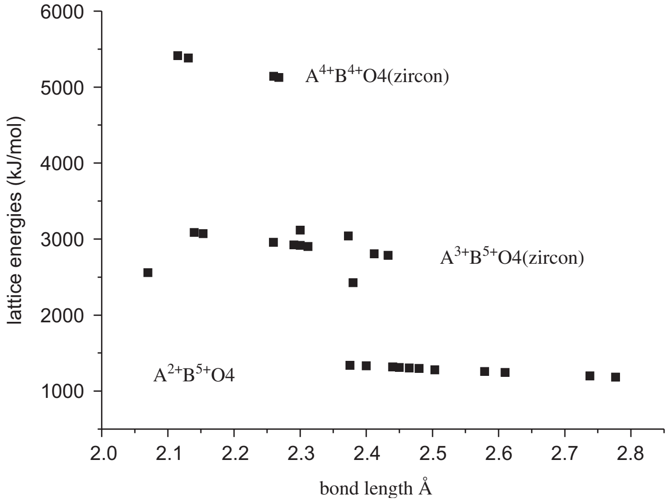

Fig. 6. The lattice energies of *A*–O bonds against *A*–O bond distances.

coefficients reduce from 11.7 ($10^{-6}\,K^{-1}$) to 3.6 ($10^{-6}\,K^{-1}$). We deduce the valence of the cation has significant effect on the magnitude of the thermal expansion of compounds with similar structures.

It can also be found that there is anisotropy in *A*–O and *B*–O bond expansions disregarding the structure families. The anisotropy is especially significant when the valence difference between *A*- and *B*-cation increases. This can trace back to the large difference in the chemical bonds lattice energies. It can be observed from the 4th column in Table 1 that all the lattice energies of *B*–O bonds are considerably larger than the lattice energies of *A*–O bonds. The lattice energies of *B*–O bonds are almost an order of magnitude larger than those of *A*–O bonds, which imply the stronger binding in *B*–O bonds compared with *A*–O bonds. This is consistent with the vibrational frequencies related to the *B*–O bonds are much greater than the vibrational frequencies of between *A* cation and BO_4

Table 3
The calculatd lattice energies (kJ/mol) of ABO_4 oxides compared with those estimated from Glasser's method

Crystals	Lattice energies from present method	Lattice energies from Glasser's method	Error
$ZrSiO_4$	26043	26293	−0.00951
$HfSiO_4$	26101	26415	−0.01188
$USiO_4$	25982	24929	0.04223
$ScPO_4$	30793	28162	0.09342
$ScVO_4$	28777	27085	0.06247
$LuAsO_4$	29118	26491	0.09918
$LuPO_4$	30537	27302	0.11849
YVO_4	28688	25979	0.10429
$ScAsO_4$	29323	27283	0.07479
YPO_4	30408	26968	0.12754
$YasO_4$	29036	26223	0.10729
$CaCrO_4$	36099	29938	0.20581
$CaWO_4$	34445	30412	0.13263
$CaMoO_4$	34564	30450	0.13512
$TbCrO_4$	28877	30100	−0.04062
$SrMoO_4$	34451	29481	0.16858
$SrWO_4$	34309	29273	0.17204
$BaWO_4$	34116	27997	0.21856
$CdMoO_4$	34863	30917	0.12764
$CdWO_4$	30543	30877	−0.01083
$NiWO_4$	30733	32532	−0.05529
$MgWO_4$	30812	32254	−0.0447
$CoWO_4$	30834	32218	−0.04297
$ZnWO_4$	30715	32083	−0.04265
$FeWO_4$	30799	32050	−0.03904
$MnWO_4$	30654	31675	−0.03222

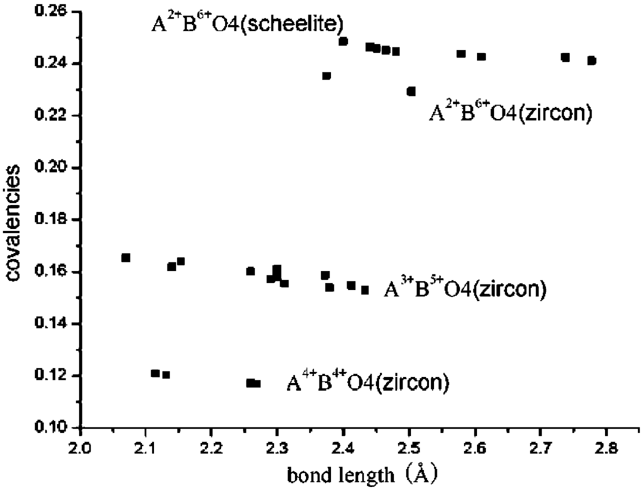

Fig. 7. The relation between the *A*–O bond covalencies and bond length.

polyhedra [30]. When the A cation valences are identical, the thermal expansion coefficients of *A*–O bonds in zircon and scheelite structures are approximately equal, larger than those in the wolframite structure. The average thermal expansion of Ca–O bonds in $CaCrO_4$ (zircon-type) and $CaWO_4$ (scheelite-type) structures are about 17.1 ($10^{-6}\,K^{-1}$), whereas the Cd–O bond expansion in $CdWO_4$ (wolframite-type structure) is 10.2 ($10^{-6}\,K^{-1}$). Archy et al [32] determined the relative average bond expansion of Ca–O from 298 to 1273 K by high-temperature X-ray diffraction, the linear expansion coefficient conversed from the relative bond expansion would be 19.4 ($10^{-6}\,K^{-1}$), and Hazen [33] proposed the relative Ca–O bond expansion to be 16.4 from an empirical relationship. The calculated Ca–O bond expansion is consistent with experimental value and data estimated from other methods. The coordination number of *A* cation decreases from eight in zircon- and scheelite-type compounds to six in wolframite-type compounds, but the coordination number of *B* cation increases from four to six. Therefore, the bond expansion of *A*–O bond decreases and the *B*–O bond expansion increases when the compound structure changes from zircon- and scheelite-type to wolframite-type structure. The expansion coefficients of zircon- and scheelite-type compounds are larger than those of wolframite-type of compounds. In summary, the cation valence and the coordination number are the principal issues affecting expansion. Hazen [33] and Megaw [34] proposed thermal expansion was related to coordination number and valence of cation, respectively. They consistently suggested bond expansion increases when the cation coordination number increases. The valences of *A*- and *B*-ion changes reversely, and the corresponding cation-oxygen bond expansion, as the *A*–O bonds expansion is the major contribution in zircon and scheelite structures, and *A*–O bonds and *B*–O bonds expansions have the equal weight contribution to the thermal expansion in the wolframite-type compounds. As a result, when the constituent elements in different structure types are equivalent, respectively, the unit cells of the zircon- and scheelite-type compounds will show more remarkable variation with increasing temperature than wolframite-type oxides. The collective influences of valence and coordination number cause the thermal expansion coefficient of wolframite-type compounds ($A^{2+}B^{6+}O_4$) are close to the $A^{3+}B^{5+}O_4$ oxides with zircon structure.

The *B*–O bonds expand more slowly when the valence of *B* cation increases and there even appear negative expansion in *B*–O bonds. Though in previous works Sleight et al. [35,36] discovered unusual negative thermal expansion in a large class of molybdates and tungstates, $A_2(BO_4)_3$ where the *B* cation is tungsten (molybdenium). They ascribed the negative thermal expansion to the transverse vibrations of bridging oxygen atoms in the compounds. Despite the structure and bond parameters (bond length, cation valence and bond covalency) similarities of the BO_4 polyhedra in these systems. In those framework compounds (negative expansion compounds), all the polyhedra are linked by just corners sharing. Nevertheless, in the ABO_4 molybdates and tungstates, the AO_8 (AO_6) and BO_4 (BO_6) polyhedra are linked sharing corners and edges, which is clearly shown in Figs. 1–3. Archy et al. [32] observed the bond distance of Mo–O bond keep nearly constant in the experimental temperature range. Hazen et al. [37] observed experimentally no W–O and Mo–O bond compression in Ca and Pb molybdates and tungstates up to 4.1 GPa, Errandonea et al. [38] verified the rigidity of the MoO_4 and WO_4 tetrahedra in $CaMoO_4$ and $CaWO_4$ under pressure till 10 GPa. Along with bearing in mind the large lattice energies of *B*–O bonds, it can be concluded that the rather strong bond between *B* cation and surrounded oxygen atoms makes *B* cation polyhedra behave as rigid unit under temperature effect. The *B*–O bond expansion would be small or even be zero when the *B*–O bonds lattice energies are great enough and the corresponding γ values are smaller than 4 ($10^{-6}\,K^{-1}$).

The expansion coefficients of compounds in the wolframite structure are predicted and shown in Table 2. To our knowledge, there is no report on the experimental investigation of the expansion behavior of compounds with the wolframite-type structure.

When analyzing the expansion coefficients of *B*–O bonds in ABO_4 oxides we are aware of the limitations of the method. Because we ascribe the unit cell expansion to the bond expansions, the bond bending effects (spatial effects) have not been considered, so the method cannot be used to abnormal expansion (negative thermal expansion) originating from the bond bending. The larger the contribution of the bond bending to the cell expansion, the error will be bigger. E.g., the estimated thermal expansion coefficient for $Sc_2(WO_4)_3$ is 1.9 ($10^{-6}\,K^{-1}$), however the measured expansion coefficient is -2.2 ($10^{-6}\,K^{-1}$) [36]. In addition, it can be found that all the calculated expansion coefficients are the mean values of crystal axes, since the unit cell expansion is obtained just from algebraic average of bond expansions, the expansion anisotropy in non-cubic solids cannot be reproduced directly. Only when the bond expansions are projected to coordinate axis with the help of the direction cosine of the bonds with respect to the coordinate axis, the coefficients along different axes are capable of compare directly with the experimental data.

4. Conclusions

The thermal expansions of zircon- and scheelite-type ABO_4 oxides were calculated and compared with experimental data. The estimated expansion coefficients are in satisfactory agreement with the experimental ones. The thermal expansion behaviors of ABO_4 oxides with wolframite and other structures were predicted. The compounds expansions in all the studied structure families come mainly from the *A*–O bond expansion. While *B* cation is high valence elements the BO_4 tetrahedra will behave as rigid unit.

Acknowledgment

This work was financially supported by the National Natural Science Foundation of China under Grant no. 20471058.

References

[1] L.E. Depero, L. Sangaletti, J. Solid State Chem. 129 (1997) 82.
[2] A. Senyshyn, H. Kraus, V.B. Mikhailik, V. Yakovyna, Phys. Rev. B 70 (2004) 214306.
[3] M. Born, K. Huang, Dynamical Theory of Crystal lattices, Oxford University Press, Oxford, 1954.
[4] A. Fleszar, X. Gonze, Phys. Rev. Lett. 64 (1990) 2961.
[5] P. Pavone, K. Karch, O. Schütt, D. Strauch, W. Windl, P. Giannozzi, et al., Phys. Rev. B 48 (1993) 3156.
[6] K. Karch, P. Pavone, W. Windl, O. Schütt, D. Strauch, Phys. Rev. B 50 (1994) 17054.
[7] R. Car, M. Parrinello, Phys. Rev. Lett. 55 (1985) 2471.
[8] Z. Gong, G.K. Horton, E.R. Cowley, Phys. Rev. B 38 (1988) 10820.
[9] Z. Gong, G.K. Horton, E.R. Cowley, Phys. Rev. B 40 (1989) 3294.
[10] R.R. Reeber, Phys. Status Solidi a 32 (1975) 321.
[11] L.G. Van Uitert, H.M. O'Bryan, M.E. Lines, H.J. Guggenheim, G. Zydzik, Mater Res. Bull. 12 (1977) 261.
[12] A.R. Ruffa, J. Mater. Sci. 15 (1980) 2258.
[13] H. Inaba, Jpn. J. Appl. Phys. 35 (1996) 3522.
[14] V. Kumar, B.S.R. Sastry, Cryst. Res. Technol. 36 (2001) 565.
[15] R.M. Finger, J. Geophys. Res. 84 (1979) 6723.
[16] L.L. Boyer, Phys. Rev. Lett. 42 (1979) 584.
[17] I. Suzuki, K. Seya, J. Phys. Earth 27 (1979) 63.
[18] Y.S. Touliukian, R.E. Taylor, T.Y.R. Lee, Thermal Expansion-non Metallic Solids, IFI/Plenum Press, New York, 1977.
[19] C. Kittel, Introduction to Solid State Physics, 3rd ed, Wiley, New York, 1966.
[20] J. Shanker, S.S. Kushwah, P. Kumar, Physica B 233 (1997) 78.
[21] D. Liu, S. Zhang, Z. Wu, Inorg. Chem. 42 (2003) 2465.
[22] S.Y. Zhang, Dielectric Chemical Bond Theory of Complex Crystals and Its Applications, Publishe, Beijing, 2005 p 161.
[23] S.Y. Zhang, H.L. Li, S.H. Zhou, T.Q. Pan, Jpn. J. Appl. Phys. 45 (2006).
[24] S.Y. Zhang, Chin, J. Chem. Phys 4 (1991) 109.
[25] Z.J. Wu, Q.B. Meng, S.Y. Zhang, Phys. Rev. B 58 (1998) 958.
[26] K. Robinson, P.H. Ribbe, Am. Miner. 56 (1971) 782.
[27] A. Zalkin, D.H. Templeton, J. Chem. Phys. 40 (1964) 501.
[28] H. Weitzel, Z. Kristallogr. 144 (1976) 238.
[29] L. Glasser, H.D.B. Jenkins, J. Am. Chem. Soc. 122 (2000) 632.
[30] E. Sarantopoulou, C. Raptis, S. Ves, D. Christofilos, G.A. Kourouklis, J. Phys.: Condens. Matter 14 (2002) 8925.
[31] M.J. Guittet, J.P. Crocombette, M. Gautier-Soyer, Phys. Rev. B 63 (2001) 125117.
[32] S.N. Achary, S.J. Patwe, M.D. Mathews, A.K. Tyagi, J. Phys. Chem. Solids 67 (2006) 774.
[33] R.M. Hazen, C.T. Prewitt, Am. Miner. 62 (1977) 309.
[34] H.D. Megaw, Mater. Res. Bull. 6 (1971) 1007.
[35] J.S.O. Evans, T.A. Mary, A.W. Sleight, J. Solid State Chem. 133 (1997) 580.
[36] J.S.O. Evans, T.A. Mary, A.W. Sleight, J. Solid State Chem. 137 (1998) 148.
[37] R.M. Hazen, L.W. Finger, J.W.E. Mariathasan, J. Phys. Chem. Solids 46 (1985) 253.
[38] D. Errandonea, J. Pellicer-Porres, F.J. Manjon, A. Segura, C. Ferrer-Roca, R.S. Kumar, et al., Phys. Rev. B 72 (2005) 174106.
[39] D. Taylor, Trans. J. Br. Ceram. Soc. 85 (1986) 147.
[40] G. Bayer, J. Less-Common Metals 26 (1972) 255.
[41] H.G. Kahle, W. Urban, W. Wühner, Phys. Status Solidi b 38 (1970) 815.
[42] H.C. Schopper, W. Urban, H. Ebel, Solid State Commun. 11 (1972) 955.
[43] V.T. Deshpande, S.V. Suryanarayana, J. Appl. Phys. 41 (1970) 422.